2011

Monoclonal antibodies for copper-64 PET dosimetry and radioimmunotherapy

Jeffrey N. Bryan
University of Missouri - Columbia

Fang Jia
University of Missouri - Columbia

Huma Mohsin
University of Missouri - Columbia

Geethapriya Sivaguru
University of Missouri - Columbia

Carolyn J. Anderson
Washington University School of Medicine in St. Louis

See next page for additional authors

RESEARCH PAPER

Cancer Biology & Therapy 11:12, 1001-1007; June 15, 2011; © 2011 Landes Bioscience

Monoclonal antibodies for copper-64 PET dosimetry and radioimmunotherapy

Jeffrey N. Bryan,[1] Fang Jia,[1] Huma Mohsin,[2] Geethapriya Sivaguru,[1] Carolyn J. Anderson,[6-8] William H. Miller,[5] Carolyn J. Henry[1,3] and Michael R. Lewis[1,4,5,9,*]

[1]Departments of Veterinary Medicine and Surgery, [2]Chemistry, [3]Internal Medicine, [4]Radiology, [5]Nuclear Science and Engineering Institute; University of Missouri-Columbia; Columbia, MO USA; [6]Mallinckrodt Institute of Radiology; [7]Department of Biochemistry and Molecular Biophysics, and [8]Chemistry; Washington University; St. Louis, MO USA; [9]Research Service; Harry S. Truman Memorial Veterans' Hospital; Columbia, MO USA

Key words: monoclonal antibodies, copper-64, positron emission tomography, tumor dosimetry, radioimmunotherapy, colon cancer, nude mice

Background: We previously described a two-antibody model of ^{64}Cu radioimmunotherapy to evaluate low-dose, solid-tumor response. This model was designed to test the hypothesis that cellular internalization is critical in causing tumor cell death by mechanisms in addition to radiation damage. The purpose of the present study was to estimate radiation dosimetry for both antibodies (mAbs) using positron emission tomography (PET) imaging and evaluate the effect of internalization on tumor growth.

Results: Dosimetry was similar between therapy groups. Median time to tumor progression to 1 g ranged from 7–12 days for control groups and was 32 days for both treatment groups ($p < 0.0001$). No statistically significant difference existed between any control group or between the treatment groups.

Material and Methods: In female nude mice bearing LS174T colon carcinoma xenografts, tumor dosimetry was calculated using serial PET images of three mice in each group of either internalizing ^{64}Cu-labeled DOTA-cBR96 (DOTA = 1,4,7,10-tetraazacyclododecane-1,4,7,10-tetraacetic acid) or non-internalizing ^{64}Cu-labeled DOTA-cT84.66 from 3 to 48 h. For the therapy study, controls (n = 10) received saline, DOTA-cBR96 or DOTA-cT84.66. Treatment animals (n = 9) received 0.890 mCi of ^{64}Cu-labeled DOTA-cBR96 or 0.710 mCi of ^{64}Cu-labeled DOTA-cT84.66. Tumors were measured daily.

Conclusions: PET imaging allows the use of ^{64}Cu for pre-therapy calculation of tumor dosimetry. In spite of highly similar tumor dosimetry, an internalizing antibody did not improve the outcome of ^{64}Cu radioimmunotherapy. Radioresistance of this tumor cell line and copper efflux may have confounded the study. Further investigations of the therapeutic efficacy of ^{64}Cu-labeled mAbs will focus on interaction between ^{64}Cu and tumor suppressor genes and copper chaperones.

Introduction

Copper-64 is a radionuclide produced by a cyclotron with an intermediate half-life ($T_{1/2}$ = 12.7 h) that decays by both β^+ (655 keV, 17.4%) and β^- (573 keV, 39.0%) emission, making it suitable for labeling monoclonal antibodies (mAbs) for positron emission tomography (PET) imaging and radioimmunotherapy (RIT) of cancer. Previous experiments in xenograft-bearing rodent models have demonstrated tumor cytotoxicity of internalizing ^{64}Cu radiopharmaceuticals superior to other nuclides, but at much lower tumor absorbed doses.

Two studies in particular offer tantalizing evidence of cytotoxicity in addition to traditional radiation damage mechanisms. Connett and others reported 82% complete tumor responses to the ^{64}Cu-labeled mAb 1A3 in Golden Syrian hamsters bearing GW39 xenografts, at a tumor absorbed dose of only 586 rad (5.86 Gy).[1] Lewis and others reported complete, but temporary, tumor remissions using the somatostatin analogue ^{64}Cu-TETA-Tyr^3-octreotate in the highly aggressive CA20948 rat pancreatic tumor model at a low tumor absorbed dose.[2] Evaluation of intracellular distribution of ^{64}Cu offers some potential insight into additional cytotoxicity mechanisms. In vivo distribution studies in rats of ^{64}Cu-TETA-octreotide demonstrated transchelation of ^{64}Cu to superoxide dismutase (SOD) in the liver.[3] Other experiments identified ^{64}Cu from ^{64}Cu-TETA-octreotide in the nucleus (19.5%) and mitochondria (21.1%) of AR42J rat pancreatic tumor cells in vitro over a 24 h period.[4] As there was no evidence that the somatostatin analogue itself had accumulated in these locations, it is possible that ^{64}Cu transchelates to copper cofactor enzymes, metalloproteins and copper-handling chaperones following internalization.

We previously reported the development and characterization of a two-antibody model for comparison of ^{64}Cu RIT.[5] We confirmed the internalization of the mAb cBR96 which recognizes the Lewis^y ceramide variant present in multiple human and veterinary carcinomas.[6,7] We also confirmed that the mAb

*Correspondence to: Michael R. Lewis; Email: LewisMic@missouri.edu
Submitted: 12/06/10; Revised: 03/04/11; Accepted: 03/17/11
DOI: 10.4161/cbt.11.12.15528

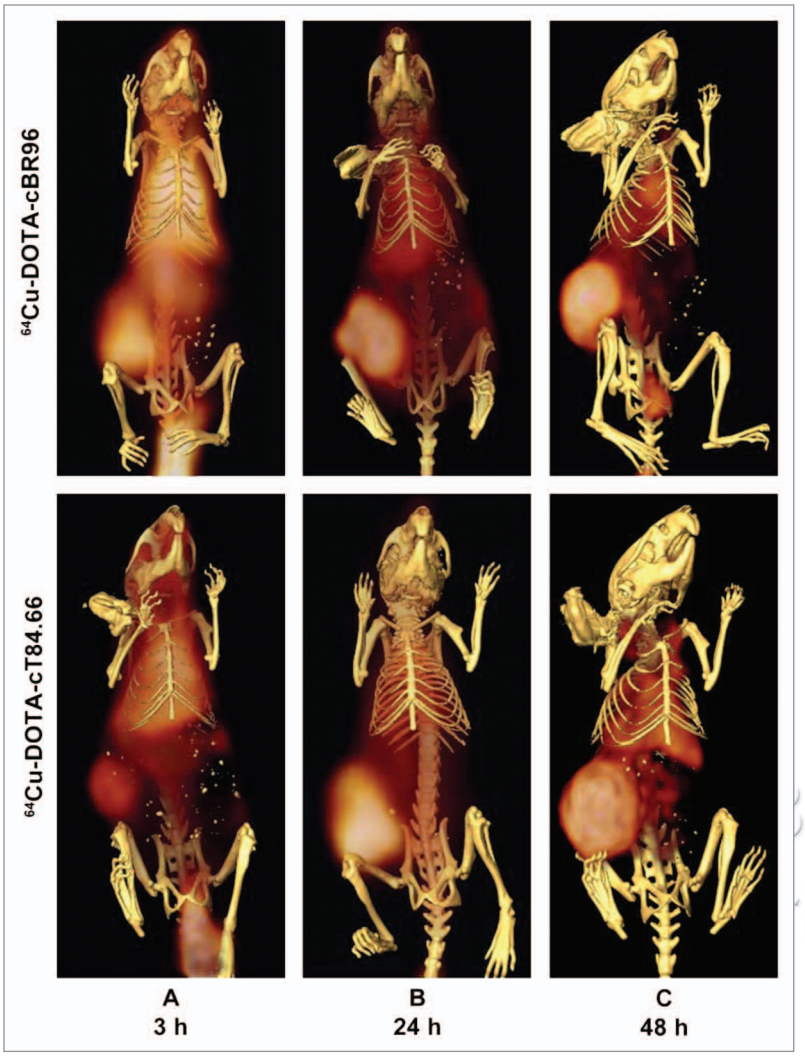

Figure 1. Representative PET/CT fusion scans at time points of approximately 3, 24 and 48 h. The ^{64}Cu-DOTA-cBR96 mice are presented above, and the ^{64}Cu-DOTA-cT84.66 mice are presented below. Note the subtle, but important, differences in the patterns of distribution to the tumor and normal organs for each mouse imaged over a 2 day period. Much more activity is visible in the tail base region for all ^{64}Cu-DOTA-cBR96 conjugates. Increased liver and intestine activity from biliary excretion is visible with ^{64}Cu-DOTA-T84.66, particularly in (C).

cT84.66,[8] which recognizes carcinoembryonic antigen (CEA) is non-internalizing.[5] This antigen is also present on numerous human carcinomas[8] and reported in veterinary hepatocellular carcinomas, rete testis mucinous adenocarcinomas and choroid plexus carcinomas.[9-11] The biodistributions of these antibodies were characterized in an LS174T nude mouse model of colon cancer and tumor dosimetry was estimated.[5]

The purpose of these experiments was to test the hypothesis that internalization of ^{64}Cu is the single necessary step in causing low-dose cytotoxicity with RIT of cancer. An imaging study was performed to test the hypothesis that the actual tumor dose received from the therapeutic administration would be equivalent between the two ^{64}Cu-labeled mAbs. A RIT experiment was performed to test our overarching hypothesis by comparing tumor response to an internalizing versus a non-internalizing mAb at the calculated tumor absorbed dose of 10 Gy in a mouse xenograft model of cancer.

Results

PET/CT imaging. Representative PET/CT images for both ^{64}Cu-labeled mAbs at time points from 3–48 h are shown in **Figure 1**. Tumor uptake was heterogeneous in most studies at the 24 and 48 h time points (**Fig. 2**). Tumor uptake of ^{64}Cu-DOTA-cBR96 was 5.06% ID/organ at 3 h, 12.38% ID/organ at 26 h and 16.12% ID/organ at 48 h. Tumor uptake for ^{64}Cu-DOTA-cT84.66 was 7.25% ID/organ at 3 h, 17.45% ID/organ at 25 h and 20.24% ID/organ at 49 h. There were no statistically significant differences between conjugates at any time point, although the power of the test is limited due to the small numbers of mice that could be imaged daily. This pattern of uptake was different from that seen in the traditional biodistribution studies in which tumor accumulation of ^{64}Cu-DOTA-cBR96 was significantly more rapid at 3 h than that of ^{64}Cu-DOTA-cT84.66. Using a Monte Carlo N-particle Transport Code,[12] the calculated absorbed dose to the tumors was 484 rad/mCi (131 mGy/MBq) for ^{64}Cu-DOTA-cBR96 and 643 rad/mCi (174 mGy/MBq) for ^{64}Cu-DOTA-cT84.66.

Qualitative analysis of the PET images revealed few regions of radioactivity accumulation that were not predicted by the traditional biodistribution studies. What did appear unexpectedly in the 3 h images for ^{64}Cu-DOTA-cBR96 was radioactivity associated with the vascular bed of the tail base. A lesser accumulation of radioactivity was visible in the tail of mice receiving ^{64}Cu-DOTA-cT84.66, likely associated with small, perivascular leakage at the injection site. This radioactivity largely washed out in both cases over the subsequent 48 h period. Minor intestinal uptake was visible in the 48 h scan of mice receiving ^{64}Cu-DOTA-cBR96. As with the traditional biodistribution studies,[5] the hepatic radioactivity of ^{64}Cu-DOTA-cT84.66 was clearly greater than that of ^{64}Cu-DOTA-cBR96. This was best illustrated by the 48 h images depicted in **Figure 1C**. Intestinal radioactivity was clearly visible in mice imaged with ^{64}Cu-DOTA-cT84.66 at 48 h.

Therapy study. The growth curves of the tumors are presented in **Figure 3**. Aggressive, unrestricted tumor growth was evident for the three control groups. Both experimental groups displayed a tumor growth delay, followed by unrestricted tumor growth. Abrupt decline in tumor volume was recorded for 22 of the 48 mice in the study. This decrease represented sudden ulceration and collapse of the tumor. The majority of these events occurred when tumor masses reached 1 g or larger. Mice were sacrificed when the tumor mass reached 3 g, the tumor developed severe ulceration or the tumor impaired the ability of the mouse to ambulate. Because of the tendency to ulcerate at a tumor burden

over 1 g, the most meaningful end point was the time to progression of tumor mass to 1 g. The Kaplan-Meier curve describing time to progression is presented in **Figure 4**. The median time to progression to 1 g ranged from 7–12 days for the three control populations. The median time to progression to 1 g was 32 days for both of the experimental groups. There was no statistically significant difference between the medians among the control groups of saline and unlabeled antibodies. The two experimental groups were also statistically indistinguishable; however, there was a statistically significant difference between the experimental and control groups ($p = 0.0001$). There was no evidence of toxicity in any of the mice in the experimental groups or the control groups receiving unlabeled mAbs.

Discussion

This therapy study yielded mixed results, some expected and some surprising. As hypothesized it is clear from the similarity between the saline control and the unlabeled DOTA-cBR96 and DOTA-cT84.66 groups that the mAbs did not initiate antibody-dependent cellular cytotoxicity (ADCC) in these animals. There was no significant difference between the times to progression to 1 g tumor mass, and no growth delay was observed in the mice receiving unlabeled antibodies compared to the mice receiving saline. Although an in vitro study previously demonstrated evidence for direct cytotoxicity as well as ADCC by unmodified BR96,[7] to our knowledge there are no in vivo experiments that confirm this effect. The lack of direct cytotoxicity or ADCC in this study may be due to ambient concentrations below those which would be optimal for cell killing or potentially due to interference with this mechanism by DOTA conjugation. In either case antibody-induced immune response did not affect the outcome of this therapy study.

What was unexpected was the lack of support for the hypothesis that internalization is the single critical step in the unusual cytotoxicity previously demonstrated for internalizing ^{64}Cu-labeled radiopharmaceuticals. Our in vitro studies confirmed the internalizing property of ^{64}Cu-DOTA-cBR96 and the non-internalizing properties of ^{64}Cu-DOTA-cT84.66.[5] However, the ^{64}Cu efflux studies previously published offer the possibility that a lack of persistence of ^{64}Cu within the cells to interact with copper chaperones after internalization may explain the lack of differential therapeutic efficacy between these two mAbs.[5] Cellular efflux has not been evaluated for ^{64}Cu- and ^{131}I-labeled 1A3 in GW39 cells, used in the experiment in which ^{64}Cu-BAT-2IT-1A3 exhibited markedly superior tumor responses (Anderson CJ, personal communication). Rapid efflux of internalized ^{64}Cu is a tempting explanation for the results of these experiments, but remains speculative as cellular efflux is difficult to quantify in vivo. What is likely, however, is that the trafficking of ^{64}Cu into the nucleus and mitochondria previously described in reference 4, would cause accumulation, and thus residualization, of radioactivity within the cells. Recently, trafficking of ^{64}Cu to the nucleus has been associated with the expression of wild-type p53.[13] The LS174T cell line expresses wild-type p53, but did not show evidence of residualization.[14] It is possible that chelation with a more stable ligand would have resulted in more favorable intracellular trafficking. Boswell and others have described a cross-bridged cyclam with greater stability than traditional chelators such as DOTA.[15] Similarly, a bombesin peptide labeled with ^{64}Cu using the chelator NOTA (NOTA = 1,4,7-triaazacyclononane-1,4,7-triacetic acid) demonstrated greater in vivo stability than a similar peptide conjugated with DOTA.[16] However, intranuclear accumulation has been reported to be inhibited by more stable chelation in at least one model.[17]

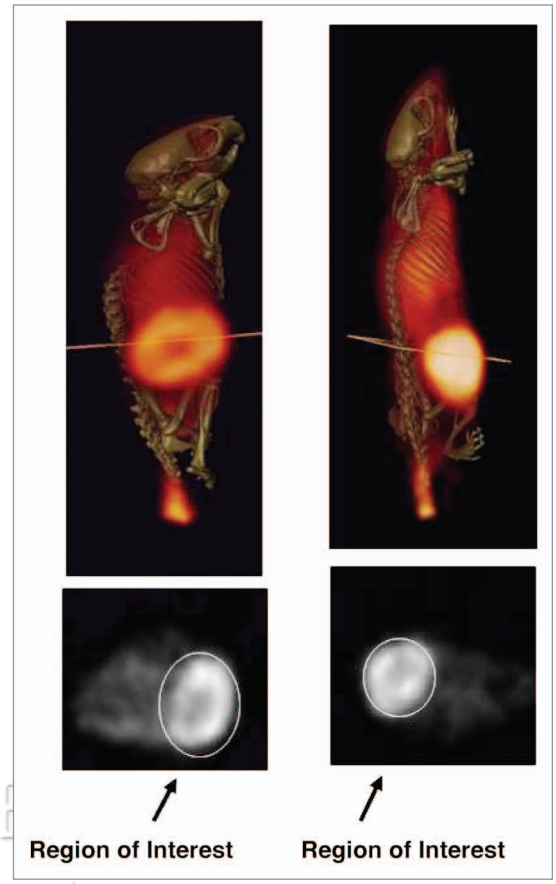

Figure 2. Representative two-dimensional slices through the tumor region for one mouse each from the ^{64}Cu-DOTA-cBR96 (left) and ^{64}Cu-DOTA-cT84.66 (right) treatment groups at 24 h. The plane depicted in the PET/CT image denotes the origin of the two-dimensional transaxial slice. The ellipse depicted denotes the region of interest of the tumor, but is not equivalent to the very precise ROI drawn around the tumor regions for PET dosimetry calculation.

The large difference in mAb dose between the biodistribution and therapy studies prompted us to confirm the tumor dosimetry by PET imaging studies. In the biodistribution experiments, different groups of mice were sacrificed at each time point. As such, mice exhibiting unusual clearance properties would be randomly distributed throughout the pool of animals, thwarting a systematic understanding of the pattern of microscopic antibody metabolism in the tumor. Furthermore, the injected dose of radiation and mAb in the biodistribution studies was nearly one log below the therapeutic dose, leaving open the possibility that a larger dose of antibody might be distributed differently.

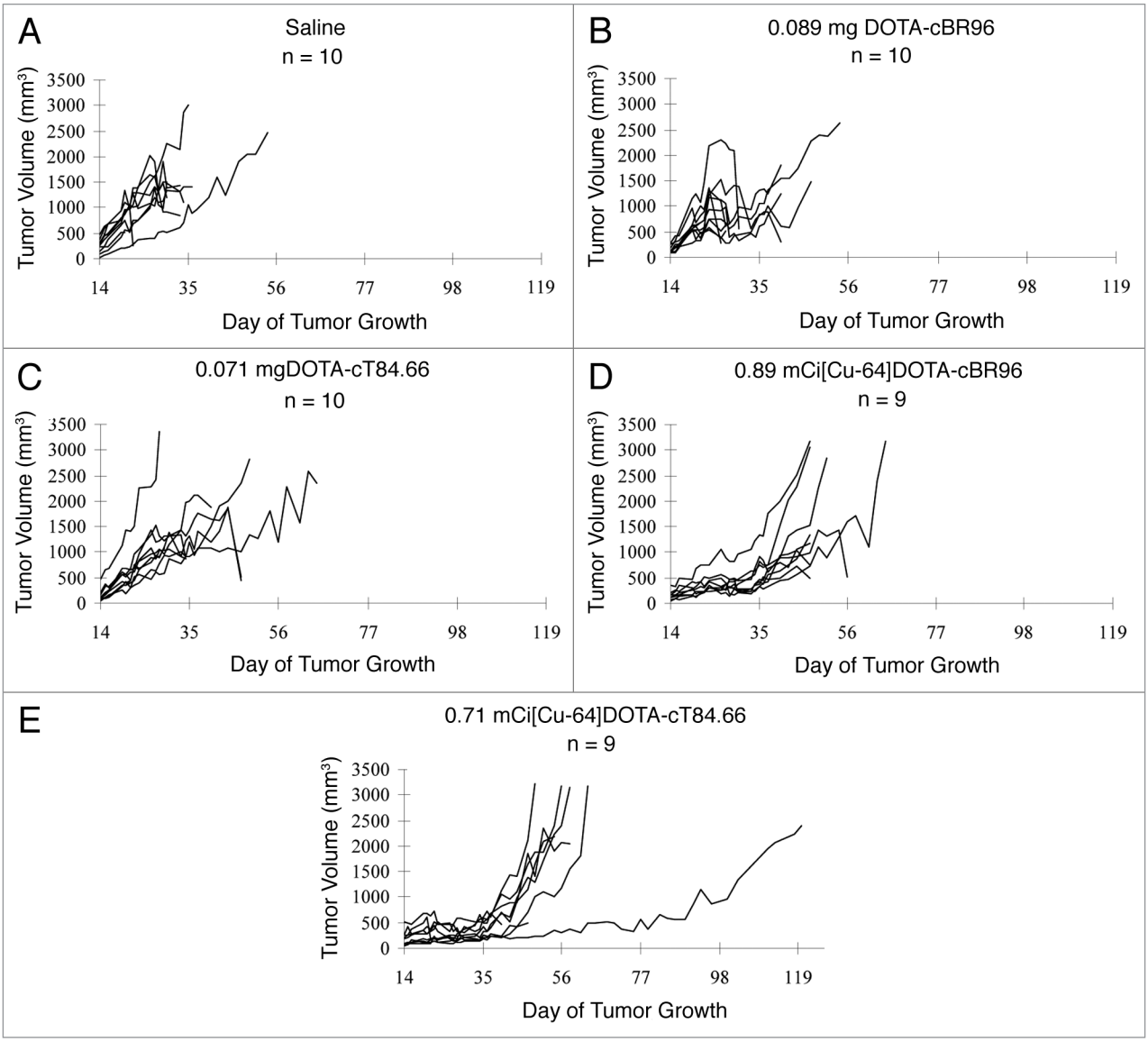

Figure 3. (A–E) Tumor growth curves for each control and experimental group. Tumor volumes are expressed in mm^3 and time is in days from treatment, after 14 days of tumor growth. Plot (A) represents the saline control mice. Plot (B) represents the unlabeled DOTA-cBR96 control mice. Plot (C) represents the unlabeled DOTA-cT84.66 control mice. Plot (D) are the ^{64}Cu-DOTA-cBR96 experimental mice. Plot (E) are the ^{64}Cu-DOTA-cT84.66 experimental mice. Large decreases in tumor volume were due to ulceration and necrosis of those tumors.

A more ideal dosimetry study would follow the distribution of the ^{64}Cu-labeled mAbs in the same group of living mice over a 48 h period. This experiment would allow a more complete understanding of the progression of distribution of the mAbs and ^{64}Cu within the animals. An animal that cleared antibody or radioactivity rapidly in the reticuloendothelial system would be identified and accounted for in the modeling of the subsequent therapy experiment. The ability to image the distribution of the ^{64}Cu-labeled mAbs with PET permits this quantification of biodistribution, including tumor targeting. Minor limitations exist in the ability to quantify the radioactivity within a region of the PET scan. However, because of the small size of the mouse, the energy of the annihilation photons detected (511 keV), as well as the subcutaneous location of the tumors, factors such as attenuation were likely to introduce negligible error into the calculations.

As previously discussed, the low abundance of β^+ emission from ^{64}Cu decay allows for efficient imaging of therapeutic doses of the radiolabeled mAbs. Thus, a full therapy dose, rather than a tracer dose, may be administered to observe biodistribution under conditions of greater mAb concentration relative to antigen pool. Qualitative evaluation of the imaging studies detected little distribution to tissue that was not predicted by the results of the sacrificial studies. However, endothelial binding of ^{64}Cu-DOTA-cBR96 in the tail vasculature was unexpected. In retrospect, this uptake may have been masked in the traditional biodistribution data because the tail was counted with the caudal half of the carcass. As with the circulating CEA pool

for ^{64}Cu-DOTA-cT84.66, the endothelial sink for deposition of radioactivity may account for the delayed tumor accumulation of ^{64}Cu-DOTA-cBR96, as detected by PET imaging, relative to the traditional biodistribution analysis.[5] Vascular endothelial binding did not appear to diminish total tumor uptake, and the tumor distribution remained similar between the two mAbs at 24 and 48 h post-injection. Minor intestinal activity was observed in mice treated with ^{64}Cu-DOTA-cBR96. Intestinal cross-reactivity with cBR96 has not been previously reported in mice.[7] It has, however, been identified in the large intestine of dogs.[6] It is not surprising that some cross-reactivity with normal tissue would exist. Consistent with sacrificial biodistribution results, ^{64}Cu-DOTA-cT84.66 demonstrated increased liver and spleen activity over time, and intestinal activity became visible at 48 h as biliary excretion of ^{64}Cu occurred. In the case of either mAb, it must be considered that copper could have been excreted into the intestinal tract unbound to antibody through the normal copper processing function of the liver. This series of non-invasive imaging studies gave striking confirmation of the biodistributions previously determined by more traditional means, with the added accuracy of repeated measures in the same living mice, and the potential to use fewer animals to obtain equivalent results.

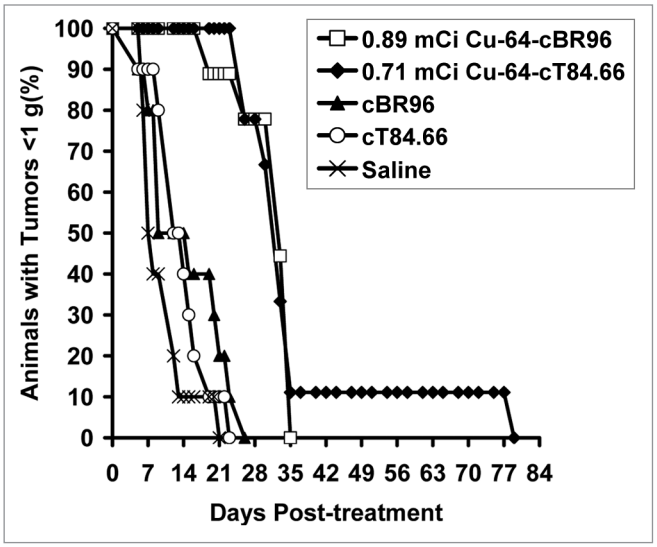

Figure 4. Kaplan-Meier plot of time to progression of tumor mass to 1 g. There was no statistically significant difference between control groups or between groups receiving ^{64}Cu. There was a significant difference between control groups and those receiving ^{64}Cu ($p < 0.0001$).

The most valuable information gained from these images, however, was to estimate tumor dosimetry based on region of interest (ROI) evaluation. Because ^{64}Cu was only available on a bi-monthly basis at the time, tumors were implanted 14 days prior to the experiment. During this time, tumors were expected to grow to approximately 200 mg in size. Prior to the imaging studies tumor growth was greater than expected, reaching 800–900 mg, four times the size of the tumors in the traditional biodistribution studies. On the two-dimensional PET images (**Fig. 2**), the tumors displayed heterogeneity of dose distribution within the parenchyma in most cases, suggesting that the large tumors had developed hypovascularized and likely necrotic areas within the tumors. Including the entire tumor area within the ROI, the larger tumors accumulated twice the radioactivity that was measured in the initial biodistribution studies. However, with four times the volume, the resulting dose to the tumors was approximately half that calculated previously. The therapy mice were injected with radiation calculated to deliver the same dose (10 Gy) to a 200 mg tumor, regardless of the mAb administered. Correcting for injected activity, for 0.89 mCi of ^{64}Cu-DOTA-cBR96, the actual dose to the tumor was 4.31 Gy, and for 0.71 mCi of ^{64}Cu-DOTA-cT84.66, the dose was 4.56 Gy in the larger tumors in the PET dosimetry experiment. Within 5% of each other, these doses are remarkably similar, given the potential for individual mouse variability, the limitations of sacrificial studies, and the great disparity in tumor size between the traditional biodistribution studies and PET imaging. Although not representative of the absolute dose administered in the therapy study, this result confirms that the dosimetry would have been similar between experimental groups in the therapy study.

PET dosimetry offers great advantages for future ^{64}Cu therapy studies. Preliminary dose-finding biodistribution studies can be accomplished using far fewer mice, and allowing statistical evaluation with repeated measures to give greater power to the analysis. When therapy studies are performed, individual mice could be screened with a tracer dose and therapeutic mass, in order to compare biodistributions, metabolism and tumor uptakes. From this test dose, the appropriate dose to deliver the desired tumor absorbed dose could be calculated, ensuring that all mice receive the intended dose. These mice could then be imaged again after the therapy dose to confirm expected distributions. Using this method, future therapy studies of ^{64}Cu-labeled delivery platforms could be better controlled, yielding more meaningful results.

In the case of this therapy study, the results of the imaging analysis suggested that the mice did, indeed, receive equivalent tumor absorbed doses from ^{64}Cu-labeled mAbs. This lends further support to the veracity of the outcome, suggesting that the hypothesis tested cannot be supported by this two-antibody system and tumor model. Although internalization appeared in previous studies to be necessary for the enhanced cytotoxicity of ^{64}Cu-labeled radiopharmaceuticals, the new information reported here suggests that cellular characteristics of copper handling or activity of apoptotic pathways may also play a large role in the cytotoxic mechanism. In vitro, LS174T cells clearly expressed mechanisms by which ^{64}Cu from both mAbs was removed from the cell into the extracellular matrix. This would be expected for a non-internalizing mAb like cT84.66, as CEA is shed continuously, but internalization of cBR96 should have resulted in residualization of radioactivity within the cell. Future evaluation of these agents must continue to focus on the fate of ^{64}Cu within the target cell.

Material and Methods

Cell line. The LS174T cell line was obtained from the American Type Culture Collection (Manassas, VA). Immediately prior

to implantation into nude mice, the cells were tested for mycoplasma and screened for a panel of 13 murine pathogens by PCR. All test results were negative, and all sentinel mice in the facility housing the nude mice tested negative for these pathogens during the course of the studies.

Animal model. The imaging and therapy studies were conducted in compliance with a protocol approved by the Animal Care and Use Committee of the University of Missouri-Columbia Animal Care Quality Assurance Office. Outbred female nu/nu mice (4–6 weeks of age) were obtained from Harlan Sprague Dawley (Indianapolis, IN). Mice were injected subcutaneously with 0.15 mL of Hank's Balanced Salt Solution containing 2 x 10^6 LS174T colon tumor cells in the right prefemoral region via a 23 gauge needle. Tumors for the imaging study reached a mean weight of 863 mg in 14 days. Tumors for the therapy study reached a mean weight of 171 mg in 14 days.

Monoclonal antibodies. The methods used to prepare the conjugates and perform quality control evaluation have been previously described in reference 5. Briefly, the antibodies used in these experiments were conjugated at a 10:1 molar ratio of DOTA-OSSu:mAb for the human/murine chimeric antibody cBR96 and a 20:1 molar ratio of DOTA-OSSu:mAb for the human/murine chimeric antibody cT84.66. The conjugates were purified by extensive dialysis against 0.1 M ammonium citrate buffer, pH 5.5. These conjugation ratios yielded 1.26 functional chelates per cBR96 mAb and 3.6 functional chelates per cT84.66 mAb.[5] Immunoreactivity and serum stability were quantitative by ELISA methods for DOTA-cBR96,[5] and by reaction with purified antigen and SE-HPLC for DOTA-cT84.66.[8]

Antibody labeling. Copper-64 was produced on a biomedical cyclotron at Washington University School of Medicine by previously published methods.[18] Conjugates were labeled with ^{64}Cu to a specific activity of 10 μCi/μg in 0.1 M ammonium citrate, pH 5.5, for 1 h at 43°C.[19] Diethylenetriaminepentaacetic acid (DTPA) was then added to a final concentration of 1 mM, and the reaction mixtures were let stand for 15 min at room temperature. The labeled mAbs were purified and exchanged into phosphate-buffered saline by gel-filtration spin column chromatography, using Bio-Spin 6 columns (Bio-Rad, Hercules, CA).[19] Specific activity of labeling was determined prior to purification and radiochemical purity was determined after purification, by SE-HPLC using a Waters (Milford, MA) Delta 600 chromatograph equipped with a manual Rheodyne injector, a Waters 2487 dual wavelength UV detector, a Packard (Downers Grove, IL) 500TR Flow Scintillation Analyzer with a GAMMA-C flow cell for ^{64}Cu, a Waters busSAT/IN analog-digital interface, and the Waters Millennium 32 software package. A Phenomenex (Torrance, CA) BioSep-SEC-S 3000 column (7.8 x 300 mm, 5 μm, 290 Å), an isocratic mobile phase of 100 mM NaH_2PO_4/0.05% NaN_3, pH 6.8 and a flow rate of 1.0 mL/min were used.

PET imaging. Fourteen days prior to the start of the study, six outbred female nu/nu mice were inoculated with LS174T cells as described above. Mice were divided into two groups (n = 3). Based on previously reported data in reference 5, respective groups received either 0.89 mCi of ^{64}Cu-DOTA-cBR96 or 0.71 mCi of ^{64}Cu-DOTA-cT84.66 intravenously via the tail vein on day 1 of the study. Mice were anesthetized with isoflurane in a Plexiglas imaging chamber and lightly immobilized with gauze. PET imaging was performed using a Philips MOSAIC high resolution rodent PET scanner and CT imaging was performed using an ImTek microCAT II scanner. Each mouse was imaged for 15–60 min by PET and for 8 min by CT at 3, 24 and 48 h post-injection.

PET tumor dosimetry. High resolution imaging data was processed using the Philips Syntegra image fusion software for co-registration of anatomic (CT) and molecular (PET) imaging. Following previously published protocols,[20,21] a region of interest (ROI) was drawn around the complete area of the tumor, and the total number of counts/pixel/min was calculated. The total counts within the tumor area were compared to the total counts within a known standard dose of ^{64}Cu for each mAb to calculate the percent injected dose to each tumor (% ID/organ) at each time point, from which the doses of radiation delivered to the tumors over the imaging period were estimated in rad/mCi and mGy/MBq. Total absorbed dose was assumed to be averaged within the tumor without attempt to separate high and low-uptake regions of the tumors. The imaging results were also evaluated subjectively for distribution of radioactivity within soft tissues of the mouse body.

Therapy study. Fourteen days prior to the start of the study, outbred female nu/nu mice were inoculated with LS174T cells as described above. Mice were divided into three control groups (n = 10) and two experimental groups (n = 9). Control groups received either 0.15 of mL saline, 0.089 mg of unlabeled DOTA-cBR96 or 0.071 mg of unlabeled DOTA-cT84.66, respectively, administered intravenously via the tail vein on day 1 of the study. A control group of ^{64}Cu-DOTA was not included, as an anticipated low calculated radiation dose would not be expected to be therapeutic if not targeted to the tumor and excretion would likely be extremely rapid. Experimental groups received either 0.89 mCi of ^{64}Cu-DOTA-cBR96 or 0.71 mCi of ^{64}Cu-DOTA-cT84.66 intravenously via the tail vein on day 1 of the study. Mice were weighed daily and examined for signs of overt systemic toxicity (e.g., weight loss >20%, lethargy, diarrhea, cyanosis). Tumors were measured in three dimensions and tumor volume calculated by the formula length x width x depth x π/6 daily until tumor growth stabilized, then three times weekly. Mice were observed for adverse reactions on a twice daily basis. Mice were sacrificed if their tumor reached 3 g, body weight decreased >20%, the tumor ulcerated or the tumor interfered with normal ambulation.

Statistical analysis. Comparison of groups in the therapy study was accomplished using a Kaplan-Meier log-rank analysis. Comparison of % ID/organ values was accomplished using one-way analysis of variance (ANOVA). Differences were deemed significant at the 95% confidence level ($p \leq 0.05$).

Acknowledgments

This research was funded in part by the University of Missouri College of Veterinary Medicine Committee on Research. The production of ^{64}Cu at Washington University School of Medicine

was supported by NIH grant R24 CA86307 from the National Cancer Institute. The authors would like to thank Dr. Clay Siegall of Seattle Genetics and Drs. John Shively and Andrew Raubitschek of City of Hope for the gifts of materials that made this research possible. The authors also acknowledge the support of the US Department of Veterans Affairs, for providing use of facilities and resources at the Harry S. Truman Memorial Veterans' Hospital in Columbia, MO.

References

1. Connett JM, Anderson CJ, Guo LW, Schwarz SW, Zinn KR, Rogers BE, et al. Radioimmunotherapy with a ^{64}Cu-labeled monoclonal antibody: a comparison with ^{67}Cu. Proc Natl Acad Sci USA 1996; 93:6814-8.
2. Lewis JS, Lewis MR, Cutler PD, Srinivasan A, Schmidt MA, Schwarz SW, et al. Radiotherapy and dosimetry of ^{64}Cu-TETA-Tyr3-octreotate in a somatostatin receptor-positive, tumor-bearing rat model. Clin Cancer Res 1999; 5:3608-16.
3. Bass LA, Wang M, Welch MJ, Anderson CJ. In vivo transchelation of copper-64 from TETA-octreotide to superoxide dismutase in rat liver. Bioconjug Chem 2000; 11:527-32.
4. Wang M, Caruano AL, Lewis MR, Meyer LA, VanderWaal RP, Anderson CJ. Subcellular localization of radiolabeled somatostatin analogues: implications for targeted radiotherapy of cancer. Cancer Res 2003; 63:6864-9.
5. Bryan JN, Jia F, Mohsin H, Sivaguru G, Miller WH, Anderson CJ, et al. Comparative uptakes and biodistributions of internalizing vs. noninternalizing copper-64 radioimmunoconjugates in cell and animal models of colon cancer. Nucl Med Biol 2005; 32:851-8.
6. Henry CJ, Buss MS, Hellstrom I, Hellstrom KE, Brewer WG, Bryan JN, et al. Clinical evaluation of BR96 sFv-PE40 immunotoxin therapy in canine models of spontaneously occurring invasive carcinoma. Clin Cancer Res 2005; 11:751-5.
7. Hellstrom I, Garrigues HJ, Garrigues U, Hellstrom KE. Highly tumor-reactive, internalizing, mouse monoclonal antibodies to Le(y)-related cell surface antigens. Cancer Res 1990; 50:2183-90.
8. Neumaier M, Shively L, Chen FS, Gaida FJ, Ilgen C, Paxton RJ, et al. Cloning of the genes for T84.66, an antibody that has a high specificity and affinity for carcinoembryonic antigen and expression of chimeric human/mouse T84.66 genes in myeloma and Chinese hamster ovary cells. Cancer Res 1990; 50:2128-34.
9. Martin de las MJ, Gomez-Villamandos JC, Perez J, Mozos E, Estrado M, Mendez A. Immunohistochemical evaluation of canine primary liver carcinomas: distribution of alpha-fetoprotein, carcinoembryonic antigen, keratins and vimentin. Res Vet Sci 1995; 59:124-7.
10. Radi ZA, Miller DL, Hines ME. Rete testis mucinous adenocarcinoma in a dog. Vet Pathol 2004; 41:75-8.
11. Cantile C, Campani D, Menicagli M, Arispici M. Pathological and immunohistochemical studies of choroid plexus carcinoma of the dog. J Comp Pathol 2002; 126:183-93.
12. Briesmiester JE. A General Monte Carlo Code N-Particle Transport Code, version 4A. LA-13709-M. Los Alamos NM, Los Alamos National Laboratory Report 2000.
13. Eiblmaier M, Meyer LA, Anderson CJ. The role of p53 in the trafficking of copper-64 to tumor cell nuclei. Cancer Biol Ther 2008; 7:63-9.
14. Violette S, Poulain L, Dussaulx E, Pepin D, Faussat AM, Chambaz J, et al. Resistance of colon cancer cells to long-term 5-fluorouracil exposure is correlated to the relative level of Bcl-2 and Bcl-X(L) in addition to Bax and p53 status. Int J Cancer 2002; 98:498-504.
15. Boswell CA, Regino CA, Baidoo KE, Wong KJ, Milenic DE, Kelley JA, et al. A novel side-bridged hybrid phosphonate/acetate pendant cyclam: synthesis, characterization and ^{64}Cu small animal PET imaging. Bioorg Med Chem 2009; 17:548-52.
16. Prasanphanich AF, Nanda PK, Rold TL, Ma L, Lewis MR, Garrison JC, et al. [^{64}Cu-NOTA-8-Aoc-BBN(7-14)NH_2] targeting vector for positron-emission tomography imaging of gastrin-releasing peptide receptor-expressing tissues. Proc Natl Acad Sci USA 2007; 104:12462-7.
17. Eiblmaier M, Andrews R, Laforest R, Rogers BE, Anderson CJ. Nuclear uptake and dosimetry of ^{64}Cu-labeled chelator somatostatin conjugates in an SSTr2-transfected human tumor cell line. J Nucl Med 2007; 48:1390-6.
18. McCarthy DW, Shefer RE, Klinkowstein RE, Bass LA, Margeneau WH, Cutler CS, et al. Efficient production of high specific activity ^{64}Cu using a biomedical cyclotron. Nucl Med Biol 1997; 24:35-43.
19. Lewis MR, Kao JY, Anderson AL, Shively JE, Raubitschek A. An improved method for conjugating monoclonal antibodies with N-hydroxysulfosuccinimidyl DOTA. Bioconjug Chem 2001; 12:320-4.
20. Anderson CJ, Dehdashti F, Cutler PD, Schwarz SW, Laforest R, Bass LA, et al. ^{64}Cu-TETA-octreotide as a PET imaging agent for patients with neuroendocrine tumors. J Nucl Med 2001; 42:213-21.
21. Wu AM, Yazaki PJ, Tsai S, Nguyen K, Anderson AL, McCarthy DW, et al. High-resolution microPET imaging of carcinoembryonic antigen-positive xenografts by using a copper-64-labeled engineered antibody fragment. Proc Natl Acad Sci USA 2000; 97:8495-500.